

## Surface Plasmon Amplification by Stimulated Emission of Radiation: Quantum Generation of Coherent Surface Plasmons in Nanosystems

David J. Bergman<sup>1,\*</sup> and Mark I. Stockman<sup>2,†</sup>

<sup>1</sup>*School of Physics and Astronomy, Raymond and Beverly Sackler Faculty of Exact Sciences, Tel Aviv University, Tel Aviv, 69978, Israel*

<sup>2</sup>*Department of Physics and Astronomy, Georgia State University, Atlanta, Georgia 30303*

(Received 15 September 2002; published 14 January 2003)

We make a step towards quantum nanoplasmonics: surface plasmon fields of a nanosystem are quantized and their stimulated emission is considered. We introduce a quantum generator for surface plasmon quanta and consider the phenomenon of surface plasmon amplification by stimulated emission of radiation (spaser). Spaser generates temporally coherent high-intensity fields of selected surface plasmon modes that can be strongly localized on the nanoscale, including dark modes that do not couple to far-zone electromagnetic fields. Applications and related phenomena are discussed.

DOI: 10.1103/PhysRevLett.90.027402

PACS numbers: 78.67.-n, 42.50.-p, 78.20.Bh, 78.45.+h

The explosive growth of nanoscience and nanotechnology during the past decade has also led to great interest and improved understanding of nanoscale optical fields, and to the development of tools for studying and exploiting them. In particular, such fields are excited at metallic nanoparticles or nanofeatures of metallic microparticles, where they are greatly enhanced due to high quality-factor surface plasmon (SP) resonances [1–3]. These local fields are singular, exhibiting giant spatial fluctuations and energy concentration in nanosize volumes [3–5]. Because of these “hot spots,” the optical responses are gigantically enhanced and can be strong enough to allow, in particular, observation of Raman scattering from a single molecule attached to a metal colloidal particle [6,7]. A promising area is local optical nanosize probing by a metal tip that creates enhanced fields in its vicinity. This was demonstrated for near-field fluorescence microscopy based on two-photon excitation [8]. A theory of manipulation of particles by enhanced optical fields at a metal tip (optical nanotweezers) was developed [9]. It was suggested, quite early, to use local fields for linear- and nonlinear-optical nanoprobng and nanomodification [10].

The above phenomena and applications are based on the excitation of local fields in a nanostructure by a resonant external optical field. Significant limitations are imposed by this mode of excitation. In particular, only a very small fraction of the excitation field energy can be concentrated in the local field. It is almost impossible to select a single mode or a few modes to excite. Also, there exist a large number of dark eigenmodes that have desirable localization properties but cannot be excited by an external wave [11]. In this Letter we propose a way to excite local fields using surface plasmon amplification by stimulated emission of radiation (spaser). The spaser radiation consists of SPs that are bosons and undergo stimulated emission but in contrast to photons can be localized on the nanoscale. Spaser as a system will

incorporate an active medium formed by two-level emitters, excited in the same way as a laser active medium: optically, or electrically, or chemically, etc. One promising type of such emitters is quantum dots (QDs). These emitters transfer their excitation energy by radiationless transitions to a resonant nanosystem that plays the same role as a laser cavity. These transitions are stimulated by the SPs already in the nanosystem, causing buildup of a macroscopic number of SPs in a single mode.

We consider a nanosystem formed by either metal or semiconductor inclusions with dielectric function  $\varepsilon(\omega)$ , embedded in a dielectric host with dielectric constant  $\varepsilon_h$ . The classical field equation for the SP eigenmodes  $\varphi_n(\mathbf{r})$  and eigenvalues  $s_n$  is [11]  $\nabla \cdot [\theta(\mathbf{r}) - s_n] \nabla \varphi_n(\mathbf{r}) = 0$ , where  $\theta(\mathbf{r})$  is the characteristic function, equal to 1 inside the inclusions and to 0 in the host.

The actual SP frequencies  $\Omega_n$  satisfy  $s(\Omega_n) = s_n$ , where  $s(\omega) \equiv [1 - \varepsilon(\omega)/\varepsilon_h]^{-1}$  is the spectral parameter [12]. These frequencies are complex,  $\Omega_n = \omega_n - i\gamma_n$ , with real frequency  $\omega_n$  and relaxation rate  $\gamma_n$  of the  $n$ th SP. For weak relaxation,  $\gamma_n \ll \omega_n$ , one finds that  $\omega_n$  satisfies an equation  $\text{Re}[s(\omega_n)] = s_n$  and that

$$\gamma_n = \frac{\text{Im}[s(\omega_n)]}{s'_n}, \quad s'_n \equiv \left. \frac{d\text{Re}[s(\omega)]}{d\omega} \right|_{\omega=\omega_n}. \quad (1)$$

Quantization of the SP system, valid in the quasistatic regime for times shorter than the SP lifetime  $\tau_n \equiv 1/\gamma_n$ , is carried out by using the following approximate expression for the energy  $H$  of an electric field  $\mathbf{E}(\mathbf{r}, t)$ , which is obtained for a dispersive system by following Ref. [13],

$$H = \frac{1}{4\pi T} \int_{-\infty}^{\infty} \frac{d[\omega \varepsilon(\mathbf{r}, \omega)]}{d\omega} \mathbf{E}(\mathbf{r}, \omega) \mathbf{E}(\mathbf{r}, -\omega) \frac{d\omega}{2\pi} d^3r. \quad (2)$$

Here  $T$  is an integration time used to calculate Fourier transforms, e.g.,  $\mathbf{E}(\mathbf{r}, \omega) = \int_{-T/2}^{T/2} \mathbf{E}(\mathbf{r}, t) e^{i\omega t} dt$ . This time should satisfy  $\tau_n \gg T \gg 1/\omega_n$ , which is possible in the

weak relaxation case, where the final results are independent of  $T$ . We expand the field operator  $\mathbf{E}(\mathbf{r}, t) \equiv -\nabla\phi(\mathbf{r}, t)$  in a series of the eigenstates  $\varphi_n(\mathbf{r})$ :

$$\phi(\mathbf{r}, t) = \sum_n \sqrt{\frac{2\pi\hbar s_n}{\varepsilon_h s'_n}} \varphi_n(\mathbf{r}) e^{-\gamma_n t} [a_n e^{-i\omega_n t} + a_n^\dagger e^{i\omega_n t}], \quad (3)$$

where  $a_n^\dagger$  and  $a_n$  are, respectively, the creation and annihilation operators of a SP in the state  $\varphi_n(\mathbf{r})$ . From Eq. (2), using Eq. (3), the quantized Hamiltonian takes on the standard harmonic oscillator form:  $H = \sum_n \hbar\omega_n (a_n^\dagger a_n + 1/2)$ .

Now assume an active host medium that we approximate as a collection of two-level dipolar emitters with population densities  $\rho_0(\mathbf{r})$  and  $\rho_1(\mathbf{r})$  in the ground and excited states, positioned at the points  $\mathbf{r}_a$ ,  $a = 1, 2, \dots$  and having dipole moments  $\mathbf{d}^{(a)}$  with the transition matrix element  $d_{10}$ . The interaction of this active medium with the SP field is described by the perturbation  $H' = \sum_a \mathbf{d}^{(a)} \cdot \nabla\phi(\mathbf{r}_a)$  to the system Hamiltonian.

Applying Fermi's golden rule to  $H'$ , and taking into account Eqs. (1) and (3), we obtain a kinetic equation governing the number  $N_n$  of SPs in the  $n$ th mode:

$$\dot{N}_n = (A_n - \gamma_n)N_n + B_n. \quad (4)$$

Assuming an isotropic distribution of the transition dipoles, we calculate the Einstein coefficient  $A_n$ , which describes the net stimulated emission of SPs:

$$A_n = \frac{4\pi s'_n s_n |d_{10}|^2 p_n q_n}{3\hbar \varepsilon_h [\text{Im}s(\omega_n)]^2} \gamma_n, \quad (5)$$

where  $p_n$  is the spatial overlap factor of the population inversion and eigenmode intensity,  $p_n = \int [|\nabla\varphi_n(\mathbf{r})|^2 \times [\rho_1(\mathbf{r}) - \rho_0(\mathbf{r})] d^3r$ . The spectral overlap factor is  $q_n = \int F(\omega) [1 + (\omega - \omega_n)^2/\gamma_n^2]^{-1} d\omega$ , where  $F(\omega)$  is the normalized-to-1 spectrum of dipole transitions in the active medium, close to its fluorescence peak. The Einstein spontaneous emission coefficient  $B_n$  is similar to  $A_n$ , but the excited state population  $\rho_1$  replaces the population inversion  $\rho_1 - \rho_0$  in the expression for  $p_n$ .

To discuss the behavior of this system, we introduce the dimensionless gain of the  $n$ th eigenmode,  $\alpha_n = (A_n - \gamma_n)/\gamma_n$ . Quantum amplification and generation of SPs exist if  $\alpha_n > 0$ . For  $\alpha_n \geq 1$ , the spontaneous emission is unimportant. In this case, coherent generation occurs, and the number of SP's in a *single eigenmode* grows exponentially fast,  $N_n \propto \exp(\gamma_n \alpha_n t)$ , eventually limited by the inversion depletion.

Consider some limiting cases. For the maximum population inversion,  $\rho_1 \gg \rho_0$ , and a thick active medium, a universal upper limit is approached,  $p_n \approx \rho$ , where  $\rho = \rho_1 + \rho_0$  is the total density of the two-level energy donors. In this case, the gain does not depend on the field distribution of individual modes, but only on their frequencies. The factor  $q_n$  depends on the width  $\Gamma$  of the

spectral function  $F(\omega)$  as compared to the SP linewidth  $\gamma_n$ : For  $\Gamma \gg \gamma_n$ ,  $q_n \approx \gamma_n/\Gamma$ , while in the opposite case  $\Gamma \ll \gamma_n$ , assuming that the donor transition is centered at the SP frequency, we have  $q_n \approx 1$ .

The SP lifetime  $\tau_n$  (mostly due to dephasing) should be long enough to enable the spaser to generate or amplify local fields; it also defines the temporal scale of the evolution of these fields [cf. Eqs. (4) and (5)]. Our numerical results reported below are for inclusions made of metallic Ag: Ag has the smallest value of  $\text{Im}(\varepsilon)$  for any natural metal in the visible and near infrared (nir) optical regions [14]; such systems therefore exhibit the largest values of  $\tau_n$ . Figure 1(a) shows calculated SP lifetimes  $\tau_n$  that are comparatively long (50–120 fs) for  $1.7 > \hbar\omega_n > 0.8$  eV. This also implies that the spaser will be relatively fast, capable of generating pulses as short as  $\leq 100$  fs.

The specific geometry of a metal/dielectric nanosystem that we consider was introduced in our previous Letter on ultrafast responses [15]. This is a flat V-shaped metallic nano-inclusion positioned in the central  $xz$  plane of the dielectric host, as illustrated in Fig. 1(b). This V shape is two grid steps (2 to 10 nm) thick in the  $y$  direction. We assume that the active host medium has a planar distribution of emitters parallel to this V-shaped inclusion and consider two cases: In a thin medium, the two-level emitters occupy the central grid plane (except for the volume occupied by the V shape itself), as well as the two neighboring grid planes above and below that plane, resulting in a total thickness of three grid steps (from 3 to 15 nm). In the opposite case of a thick medium, the emitters occupy all the host volume. In all cases we assume  $\rho_1 = \rho$  and  $q_n = 1$ , as already discussed.

Emission in the nir, where spasing is expected, imposes stringent requirements on the two-level emitters. Infrared dyes are inefficient and not very stable at room temperature. Two other possibilities are rare-earth ions and semiconductor QDs. The latter seem the most promising, since they are tunable in frequency due to quantum confinement, have relatively large transition dipoles  $d_{10}$  and narrow transition lines, and allow dense packing without compromising their optical properties [16]. The well-studied CdSe QDs emit at visible frequencies, too

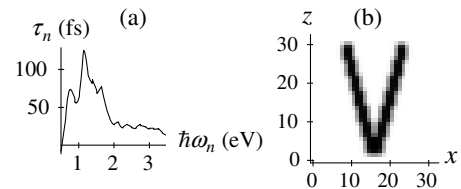


FIG. 1. (a) SP lifetime  $\tau_n = 1/\gamma_n$  as a function of SP eigenenergy  $\hbar\omega_n$ ; computed from Eq. (1). (b) V-shaped nanosized metallic inclusion in the  $xz$  plane. Distances are expressed as grid steps, with one step corresponding to a distance of 1 to 5 nm. The lower limit allows us to use a macroscopic permittivity, while the upper limit satisfies the requirement that the entire system size should be on the nanoscale.

high for the spaser medium. The novel PbS and PbSe QDs can be synthesized with radii  $R_D = 1\text{--}8$  nm to have transition energies  $0.7\text{--}1.8$  eV (see, e.g., Refs. [17,18]), which are ideally suited for spasing.

The dipole element for the  $1S_e \rightarrow 1S_h$  transition in QDs can be estimated from Kane's theory, conventionally assuming strong overlap of the envelope states, as  $d_{10} = e\sqrt{fK}/(2m_0\omega_n^2)$ , where  $f$  is the transition oscillator strength,  $K \approx 3$  eV is Kane's interband parameter, and  $m_0$  is the bare electron mass. Setting  $f \approx 1$ , which somewhat underestimates  $d_{10}$  as well as the consequent gain, we obtain  $d_{10} = 1.9 \times 10^{-17}$  esu.

We estimate  $\varepsilon_h$  from the Maxwell Garnett formula assuming a dense packing of QDs in vacuum and adopting the known value of  $\approx 23$  for the dielectric constant of PbS and PbSe, obtaining  $\varepsilon_h = 6.6$ . The QD spectral width  $\Gamma$  is mostly due to the inhomogeneous broadening. In chemically synthesized QDs [16],  $\Gamma$  is small enough,  $\Gamma \sim \gamma_n$ , yielding  $q_n \lesssim 1$ , which is sufficient for spasing.

Because both  $d_{10}$  and  $\varepsilon_h$  are essentially independent of the QD size, Einstein's stimulated emission coefficient  $A_n$  in Eq. (5) and, consequently, the spaser gain  $\alpha_n$  are higher for smaller QDs,  $A_n \propto \rho \propto R_D^{-3}$ . For our computations, we chose a moderately small  $R_D = 2.3$  nm, to be on the conservative side in estimating the gain.

The spaser gain  $\alpha_n$  is displayed in Fig. 2 vs  $\hbar\omega_n$  for both a thick and a thin medium. High values of  $\alpha_n$ , up to 12, are predicted for the latter [panel (b)]. The maximum value of  $\alpha_n$  is even greater for the thick medium, and the amplification spectral band is wider [panel (a)]. The similarity in response of these two samples is due to the strong localization near the metal surface of the efficient spasing modes: only those QDs contribute that are positioned in the areas filled by these modes. The large gain for a thin (a few monolayers) QD active medium which surrounds the metal inclusion is advantageous: a spaser is possible whose total size is on the nanoscale.

In a thin active medium [Fig. 2(b)], the function  $\alpha_n(\hbar\omega_n)$  exhibits some irregularities ("noise"). These come from fluctuations of the overlap factor  $p_n$  from mode to mode, illustrated in Fig. 3(a), which reflect the chaotic nature of these modes. Fortunately, the gain is maximal for  $\hbar\omega_n$  between 1.1 and 1.9 eV, where these fluctuations are small. When Au replaces Ag, computations indicate (data not shown) a positive gain  $\alpha_n$  only if

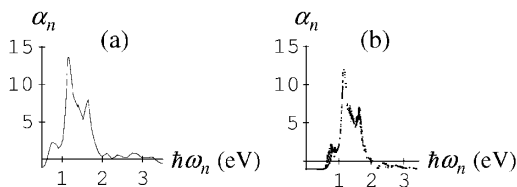


FIG. 2. Gain  $\alpha_n$  of spaser as a function of the eigenmode energy  $\hbar\omega_n$ . (a) Thick active medium,  $p_n = \rho$ . (b) Thin active medium; see text.

027402-3

$R_D < 2$  nm, and  $\alpha_n$  values that are significantly smaller. This is due to the higher losses in Au.

As we showed previously, there exist dark eigenmodes which cannot be excited or observed from the far field (wave) zone [11]. Among them are all the Anderson-localized eigenmodes. An important question is whether these dark eigenmodes can be excited (generated) in spaser. This is not only a principal fundamental question but is also of significant importance for applications: Strongly localized dark eigenmodes excited in a spaser are promising for nanometer probing and high-field nanoscale photomodification.

The ability of the spaser to excite both luminous and dark eigenmodes, including the strongly localized ones, is clearly demonstrated by the data of Fig. 3(b) where we plot the gain factor  $\alpha_n$  vs the oscillator strength  $f_n$  for every eigenmode. The eigenmodes with  $f_n < 10^{-7}$  can be considered as dark, and those with  $f_n \geq 10^{-7}$  as luminous. From Fig. 3(b), we conclude that the highest-gain eigenmodes ( $\alpha_n \geq 10$ ) are quite rare and almost equally divided between dark and luminous.

When the spaser amplification condition  $\alpha_n > 0$  is satisfied, a generating  $n$ th eigenmode accumulates a macroscopic number  $N_n$  of coherent SPs, which induces a local field of root-mean-square (RMS) magnitude

$$E(\mathbf{r}) = \langle [\nabla \phi(\mathbf{r})]^2 \rangle^{1/2} = E_n(\mathbf{r})(N_n + 1/2)^{1/2},$$

$$E_n(\mathbf{r}) = \{4\pi\hbar s_n [\nabla \varphi_n(\mathbf{r})]^2 / \varepsilon_h s_n'\}^{1/2}. \quad (6)$$

In Fig. 4, we show the RMS amplitude  $E_n(\mathbf{r})$  in the metal nanostructure plane for eigenmodes with the highest spaser gains at the two spectral maxima  $\hbar\omega_n \approx 1.16$  eV [panels (a) and (b)], and  $\hbar\omega_n \approx 1.6$  eV [panels (c) and (d)]. The highest gain occurs for a luminous eigenmode [panel (a)] with  $\hbar\omega_n = 1.15$  eV [cf. Figs. 1 and 2]. This eigenmode is concentrated within a radius  $a \approx 15$  nm around the tip of the V shape. The spasing of this mode will be seen in the far zone as almost isotropic radiation with an anomalously narrow spectrum (high temporal coherence) and high spectral intensity. A dense enough ensemble of spasers may actually form a laser developing also spatial coherence, which we will discuss elsewhere.

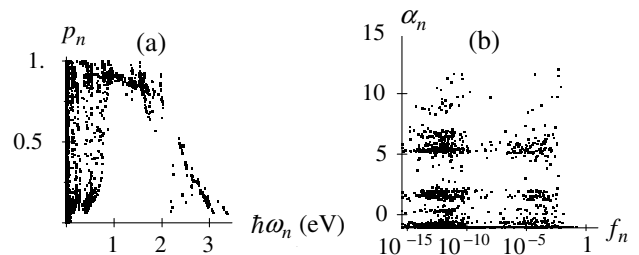


FIG. 3. (a) Overlap factor  $p_n$  as a function of the mode energy  $\hbar\omega_n$ . (b) Amplification gain  $\alpha_n$  vs eigenmode oscillator strength  $f_n$ .

027402-3

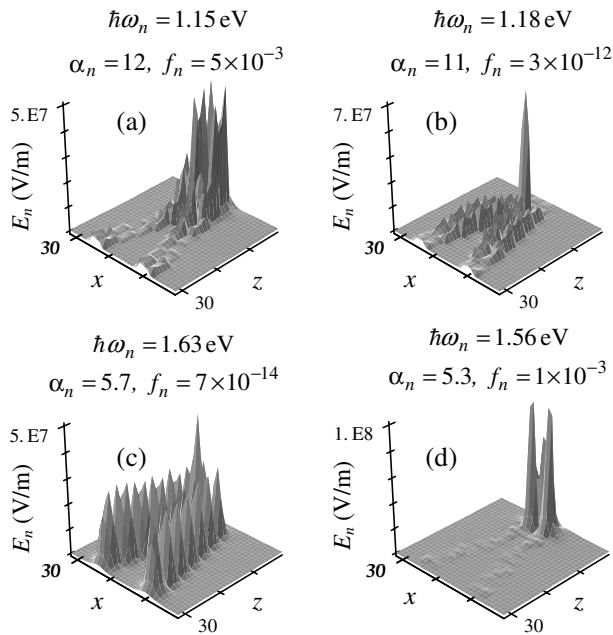


FIG. 4. Local field amplitude in the V-shaped inclusion plane for eigenmodes with highest gains in the regions of two spectral maxima for the case of thin active medium. The inclusion material is Ag. The grid step is assumed to be 2 nm.

Another high gain spaser eigenmode at  $\hbar\omega_n = 1.18$  eV, displayed in Fig. 4(b), is a completely dark eigenmode that creates very high local fields of  $\approx 7 \times 10^7 (N_n + \frac{1}{2})^{1/2}$  V/m, which are only a few orders of magnitude below atomic-strength fields. These fields are sharply localized at the tip of the nanostructure providing a unique tool for possible applications in nanoscale optical probing and modification where the undesirable, background far-zone radiation from the tip itself is absent.

In the second spectral maximum, the spaser eigenmodes at  $\hbar\omega_n = 1.63$  eV [Fig. 4(c)] and 1.56 eV [Fig. 4(d)] are similar in some but not all respects to those in panels (a) and (b) discussed above: A dark eigenmode at 1.63 eV is now delocalized, while a luminous eigenmode at 1.56 eV is strongly localized at the tip. However, the gains of these eigenmodes are about half of those at  $\approx 1.16$  eV. Note that the selection of this vs the previous group of eigenmodes can be done by tuning the transition frequency of QDs by selecting their sizes. At a given frequency, an eigenmode can be selected by positioning QDs in the region where its local fields are maximal.

The present quantum-plasmonics theory may have applications other than spaser. One such application is based on the fact that the Hamiltonian is a functional of the system geometry on the nanoscale, namely,  $H = \sum_n \hbar\omega_n [\theta(\mathbf{r})] (N_n + \frac{1}{2})$ . This brings about mechanical stresses in the system which depend on the level of excitation, but exist even for  $N_n = 0$  (Casimir effect).

To summarize, we proposed the spaser effect and prospective quantum-nanoplasmonic device. Spaser is not a laser: Its two-level emitters (QDs, in particular) do not emit light waves but rather undergo *radiationless transitions* where their excitation energy is transformed into quasistatic electric field energy of SPs. The stimulated nature of this energy transfer causes buildup of macroscopic numbers of coherent SPs in individual eigenmodes of a nanosystem. It is possible to generate dark SPs that do not couple to far-zone fields. Spaser generates intense, nanoscale-localized optical-frequency fields with many possibilities for prospective applications in nanoscience and nanotechnology, in particular, for near-field nonlinear-optical probing and nanomodification.

This work was supported by the Chemical Sciences, Biosciences and Geosciences Division of the Office of Basic Energy Sciences, Office of Science, U.S. Department of Energy. Partial support for the work of D.J.B. was provided by grants from the U.S.–Israel Binational Science Foundation and the Israel Science Foundation. M. I. S. is grateful to V. I. Klimov for highly valuable consultations on QDs and to J. E. Sipe for discussions of field quantization approaches.

\*Electronic address: bergman@post.tau.ac.il

†Electronic addresses: mstockman@gsu.edu;

<http://www.phy-astr.gsu.edu/stockman>

- [1] V. M. Shalaev and M. I. Stockman, Zh. Eksp. Teor. Fiz. **92**, 509 (1987) [Sov. Phys. JETP **65**, 287 (1987)]; A. V. Butenko, V. M. Shalaev, and M. I. Stockman, Zh. Eksp. Teor. Fiz. **94**, 107 (1988) [Sov. Phys. JETP **67**, 60 (1988)].
- [2] M. I. Stockman *et al.*, Phys. Rev. B **46**, 2821 (1992).
- [3] M. I. Stockman *et al.*, Phys. Rev. Lett. **72**, 2486 (1994).
- [4] M. I. Stockman, L. N. Pandey, and T. F. George, Phys. Rev. B **53**, 2183 (1996).
- [5] S. Gréillon *et al.*, Phys. Rev. Lett. **82**, 4520 (1999).
- [6] K. Kneipp *et al.*, Phys. Rev. Lett. **78**, 1667 (1997).
- [7] S. Nie and S. R. Emory, Science **275**, 1102 (1997).
- [8] E. J. Sánchez, L. Novotny, and X. S. Xie, Phys. Rev. Lett. **82**, 4014 (1999).
- [9] L. Novotny, R. X. Bian, and X. S. Xie, Phys. Rev. Lett. **79**, 645 (1997).
- [10] M. I. Stockman, Autometria **3**, 30 (1989) [Optoelectron. Instrum. Data Process. **3**, 27 (1989)].
- [11] M. I. Stockman, S. V. Faleev, and D. J. Bergman, Phys. Rev. Lett. **87**, 167401 (2001).
- [12] D. J. Bergman and D. Stroud, Solid State Phys. **46**, 148 (1992).
- [13] L. D. Landau and E. M. Lifshitz, *Electrodynamics of Continuous Media* (Pergamon, Oxford, New York, 1984), Chap. 9, Sec. 80.
- [14] P. B. Johnson and R. W. Christy, Phys. Rev. B **6**, 4370 (1972).
- [15] M. I. Stockman, S. V. Faleev, and D. J. Bergman, Phys. Rev. Lett. **88**, 067402 (2002).
- [16] V. I. Klimov *et al.*, Science **290**, 314 (2000).
- [17] A. Lipovskii *et al.*, Appl. Phys. Lett. **71**, 3406 (1997).
- [18] K. Wundke *et al.*, Appl. Phys. Lett. **76**, 10 (2000).